INVERSE KINEMATICS OF A PARALLEL FLIGHT SIMULATOR

Stefan STAICU[1], Constantin OCNARESCU[2], Liviu Marian UNGUREANU[3]

Recursive matrix relations for kinematics analysis of a parallel manipulator, namely the spatial flight simulator, is established in this paper. Knowing the general motion of the platform, the inverse kinematics problem is solved based on the connectivity relations. Finally, some simulation graphs for the input displacements, velocities and accelerations are obtained.

Keywords: Connectivity relations; Flight simulator, Kinematics, Parallel robot

1. Introduction

Parallel manipulators consist, in general, of two main bodies coupled via numerous legs acting in parallel. The links of the robot are connected one to the other by spherical joints, universal joints, revolute joints or prismatic joints. The number of actuators is typically equal to the number of degrees of freedom and each leg is controlled at or near the fixed base [1]. Theses mechanisms can be found in practical applications, in which it is desired to orient a rigid body in space of high speed, such as flight simulators [2], [3], [4], [5] and positional trackers [6], [7]. A first spatial robot used in the amusement parks was built in 1928 by James E. Gwinnett [8] and was patented as a simulator by Ga1anov and Diaciun [9].

In the present paper, a recursive matrix method is applied to the inverse kinematics analysis of a spatial 3-DOF parallel mechanism, to prove that the number of equations and computational operations reduces significantly by using a set of matrices for kinematics modelling.

2. Kinematics analysis

The parallel manipulator has a spatial structure and is used as a flying simulator in the amusement parks. Additionally, a closed cab with two doors is

[1] Professor, Department of Mechanics; University POLITEHNICA of Bucharest, ROMANIA, e-mail: staicunstefan@yahoo.com
[2] Professor, Department of Mechanisms Theory and Robotics, University POLITEHNICA of Bucharest, ROMANIA
[3] Assistant, Department of Mechanisms Theory and Robotics, University POLITEHNICA of Bucharest, ROMANIA, e-mail: ungureanu.liviu.marian@gmail.com

placed on the moving platform (Fig. 1). The architecture of the robot consists of a fixed triangular base $A_1B_1C_1$ and an upper moving platform $A_4B_4C_4$ that is a rectangle with b and h the lengths of the geometric characteristics, two passive legs and three active extensible legs. The first active leg A is typically contained within the Ox_0y_0 median vertical plane of the cab platform, whereas the remaining active legs B, C are starting from a perpendicular vertical plane, symmetrically placed relatively to the median plane. Provided with identical kinematical structure, these last active limbs connect the fixed base to the moving platform by two universal (U) joints interconnected through a prismatic ($\underline{P}$) joint made up of a cylinder and a piston. Hydraulic or pneumatic systems can be used to vary the lengths of the prismatic joints and to control the location of the platform. There are three active prismatic joints A_2, B_3, C_3, four passive universal joints B_1, B_4, C_1, C_4, seven passive revolute joints $A_1, A_3, A_4, D_1, D_2, E_1, E_2$ and one internal passive prismatic pair jointed at the point E_2.

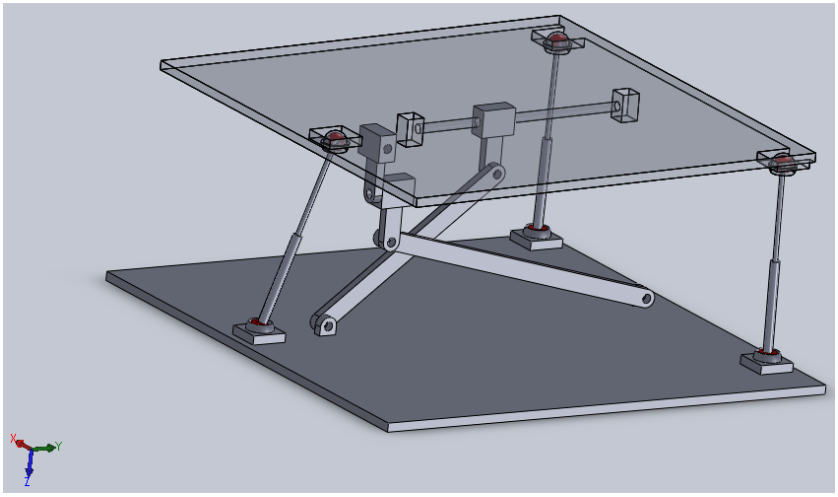

Fig. 1 Parallel flight simulator

For the purpose of analysis, we assign a fixed Cartesian coordinate system $Ox_0y_0z_0(T_0)$ at the point O of the fixed base platform and a mobile frame $Gx_Gy_Gz_G$ attached on the mobile platform at its characteristic point G. Grübler mobility equation predicts that the device has certainly three degrees of freedom.

The moving platform is initially located at a *central configuration*, where the platform is not rotated with respect to the fixed base and the point G is located at an elevation h_G. We also consider that the three sliders A_2, B_3, C_3 are initially starting from the positions $A_1A_2 = s_A, B_2B_3 = s_B, C_2C_3 = s_C$ (Fig. 2). .

To simplify the graphical image of the kinematical scheme of the mechanism, in what follows we will represent the intermediate reference systems by only two axes, so as is used in most of robotics papers [1], [2], [10]. It is noted that the relative rotation with angle $\varphi_{k,k-1}$ or the relative translation of the body T_k with the displacement $\lambda_{k,k-1}$ must always be pointed along the direction of the z_k axis.

The leg A consists of a fixed revolute joint, a moving cylinder which has a rotation about z_1^A axis with the angle φ_{10}^A and the angular velocity $\omega_{10}^A = \dot{\varphi}_{10}^A$. A prismatic joint is as well as a piston of length l_1 linked at the $A_2 x_2^A y_2^A z_2^A$ frame, having a relative motion with the displacement λ_{21}^A and the velocity $v_{21}^A = \dot{\lambda}_{21}^A$. A new revolute joint is introduced at a homogenous rod of length h linked at the $A_3 x_3^A y_3^A z_3^A$ frame, having a perpendicular rotation about z_3^A axis with the angle φ_{32}^A and the angular velocity $\omega_{32}^A = \dot{\varphi}_{32}^A$. Finally, the median axis of the moving platform rotates around the rod A_3G with the angle φ_{43}^A and the angular velocity $\omega_{43}^A = \dot{\varphi}_{43}^A$.

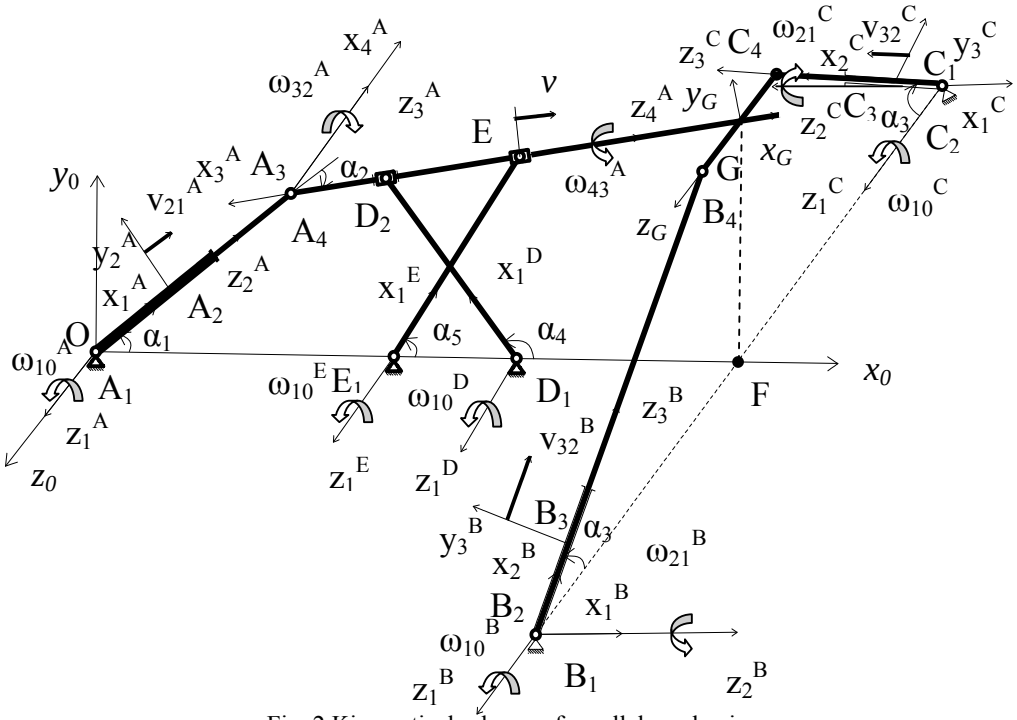

Fig. 2 Kinematical scheme of parallel mechanism

Concerning other two active kinematical chains, the architecture of the leg B, for example, consists of the cross of a fixed Hooke joint linked at the

frame $B_1x_1^By_1^Bz_1^B$, characterised by absolute angle of rotation φ_{10}^B and the angular velocity $\omega_{10}^B=\dot{\varphi}_{10}^B$, connected at a moving cylinder $B_2x_2^By_2^Bz_2^B$, which has a relative rotation around $B_2z_2^B$ axis with the angle φ_{21}^B, so that $\omega_{21}^B=\dot{\varphi}_{21}^B$. An actuated prismatic joint is as well as a piston of length l_2 linked to the $B_3x_3^By_3^Bz_3^B$ frame, having a relative displacement λ_{32}^B and velocity $v_{32}^B=\dot{\lambda}_{32}^B$. Finally, a second universal joint B_4 is introduced at the apex of the rectangular moving platform.

Additionally, two rigid cranks jointed at two fixed revolute pairs D_1, E_1 execute oscillating rotations with the angles $\varphi_{10}^D, \varphi_{10}^E$ and the angular velocities $\omega_{10}^D, \omega_{10}^E$, respectively. Finally, the internal prismatic pair E_2 starts from an initial position $D_2E_2=s$, having the relative displacement λ and the velocity $v=\dot{\lambda}$.

Starting from the reference origin O and pursuing along five independent legs $OA_1A_2A_3A_4$, $OB_1B_2B_3$, $OC_1C_2C_3$, OD_1, OE_1, we obtain following transformation matrices

$$\begin{aligned} &a_{10}=a_{10}^{\varphi}a_1^{\alpha},\ a_{21}=\theta,a_{32}=a_{32}^{\varphi}a_2^{\alpha}\theta,\ a_{43}=a_{43}^{\varphi}\theta^T,b_{10}=b_{10}^{\varphi},\ b_{21}=b_{21}^{\varphi}a_3^{\alpha}\theta,b_{32}=\theta \\ &c_{10}=c_{10}^{\varphi},\ c_{21}=c_{21}^{\varphi}a_3^{\alpha}\theta^T,c_{32}=\theta,\ d_{10}=d_{10}^{\varphi}a_4^{\alpha},\ e_{10}=e_{10}^{\varphi}a_5^{\alpha}, \end{aligned} \tag{1}$$

where we denote the matrices:

$$a_i^{\alpha}=rot(z,\alpha_i),\ \theta=rot(y,\pi/2),\ p_{k,k-1}^{\varphi}=rot(z,\varphi_{k,k-1})\ \ (p=a,b,c,d,e). \tag{2}$$

A complete description of the absolute position and orientation of the platform requires four variables: the coordinates x_0^G, y_0^G of the point G and two Euler's angles ψ, ϕ associated with two successive orthogonal rotations. Since all rotations take place successively about the moving coordinate axes, the general rotation matrix $R=R_{21}R_{10}$ is obtained by multiplying two known transformation matrices

$$R_{10}=rot(z,\psi+\alpha_1-\alpha_2),\ \ R_{21}=rot(x,\phi). \tag{3}$$

Here, x_0^G, y_0^G and ϕ are chosen as the independent variables and ψ is a parameter of a *parasitic* motion. The parasitic motion from the four motions of the moving platform is permanently dependent on the independent variables.

The conditions concerning the absolute orientation of the moving platform are given by the following matrix identity

$$\theta^T a_{40}=R, \tag{4}$$

from which we obtain significant relations between the angles of rotation

$$\psi = \varphi_{10}^{A} - \varphi_{32}^{A}, \phi = \varphi_{43}^{A}. \tag{5}$$

In the inverse geometric problem, the position of the mechanism is completely given through three variables x_0^G, y_0^G, ϕ. For the parallel simulator, the rotation angle ϕ is the only *completely independent* variable with other three pose parameters.

Consider, for example, that during three seconds the rotation of the moving platform around its median axis and the motion of the characteristic point G along a *rectilinear trajectory* are expressed in the fixed frame $Ox_0y_0z_0$ through the following analytical functions

$$\frac{x_0^G - (d_2 + d_3 + d_4)}{x_0^{G*}} = \frac{y_0^G - h_G}{y_0^{G*}} = \frac{\phi}{\phi^*} = 1 - \cos\frac{\pi}{3}t, \tag{6}$$

where the values $2x_0^{G*}, 2y_0^{G*}, 2\phi^*$ denote the final position and orientation of the moving platform.

A set of 12 independent variables $\varphi_{10}^A,\ \lambda_{21}^A,\ \varphi_{32}^A,\ \varphi_{10}^B,\ \varphi_{21}^B,\ \lambda_{32}^B,\ \varphi_{10}^C,\ \varphi_{21}^C,\ \lambda_{32}^C,\ \varphi_{10}^D,\ \varphi_{10}^E,\ \lambda$ will be determined by vector-loop equations [11]

$$\begin{aligned}
&\vec{r}_{10}^{\,A} + \sum_{k=1}^{3} a_{k0}^T \vec{r}_{k+1,k}^{\,A} + a_{40}^T r_4^G = \vec{r}_{10}^{\,B} + \sum_{k=1}^{2} b_{k0}^T \vec{r}_{k+1,k}^{\,B} + b_{30}^T \vec{r}_3^{\,B_4} - a_{40}^T \vec{r}_4^{\,GB_4} = \\
&= \vec{r}_{10}^{\,C} + \sum_{k=1}^{2} c_{k0}^T \vec{r}_{k+1,k}^{\,C} + c_{30}^T \vec{r}_3^{\,C_4} - a_{40}^T \vec{r}_4^{\,GC_4} = \vec{r}_{10}^{\,D} + d_{10}^T \vec{r}_1^{\,D_2} + a_{30}^T \vec{r}_3^{\,D_2G} = \\
&= \vec{r}_{10}^{\,E} + e_{10}^T \vec{r}_1^{\,E_2} + a_{30}^T \vec{r}_3^{\,E_2G} = \vec{r}_0^{\,G},
\end{aligned} \tag{7}$$

Where

$$\begin{aligned}
&\vec{r}_{10}^{\,A} = \vec{0}, \vec{r}_{21}^{\,A} = (s_A + \lambda_{21}^A)\vec{u}_1, \vec{r}_{32}^{\,A} = l_1\vec{u}_3, \vec{r}_{43}^{\,A} = \vec{0}, \vec{r}_4^{\,G} = h\vec{u}_3, \vec{u}_1 = [1 \quad 0 \quad 0]^T, \vec{u}_3 = [0 \quad 0 \quad 1]^T \\
&\vec{r}_{10}^{\,B} = [d_2 + d_3 + d_4 \quad 0 \quad d_5]^T, \vec{r}_{21}^{\,B} = \vec{0}, \vec{r}_{32}^{\,B} = (s_B + \lambda_{32}^B)\vec{u}_1, \vec{r}_3^{\,B_4} = l_2\vec{u}_3, \vec{r}_4^{\,GB_4} = -\frac{1}{2}b\vec{u}_1 \\
&\vec{r}_{10}^{\,C} = [d_2 + d_3 + d_4 \quad 0 \quad -d_5]^T, \vec{r}_{21}^{\,C} = \vec{0}, \vec{r}_{32}^{\,C} = (s_C + \lambda_{32}^C)\vec{u}_1, \vec{r}_3^{\,C_4} = l_2\vec{u}_3, \vec{r}_4^{\,GC_4} = \frac{1}{2}b\vec{u}_1 \\
&\vec{r}_{10}^{\,D} = (d_2 + d_3)\vec{u}_1, \vec{r}_1^{\,D_2} = l_3\vec{u}_1, \vec{r}_3^{\,D_2G} = (d_1 - h)\vec{u}_1, \vec{r}_{10}^{\,E} = d_2\vec{u}_1, \vec{r}_1^{\,E_2} = l_4\vec{u}_1, \vec{r}_3^{\,E_2G} = (s + d_1 - h + \lambda)\vec{u}_1
\end{aligned} \tag{8}$$

From the vector equations (7) we obtain 12 analytical equations for the inverse geometric solution, giving the expressions of all 12 above independent variables.

The motions of the component elements of the manipulator are characterized by the relative velocities of the joints, the relative angular velocities and their *associated* skew-symmetric matrices

$$\vec{v}_{k,k-1} = \dot{\lambda}_{k,k-1}\vec{u}_3\,,\ \vec{\omega}_{k.k-1} = \dot{\varphi}_{k,k-1}\vec{u}_3\,,\ \ \widetilde{\omega}_{k,k-1} = \dot{\varphi}_{k,k-1}\widetilde{u}_3\,. \tag{9}$$

Deriving the relations (5) and the geometrical constraints (7), we obtain first the angular velocity $\omega_{43}^A = \dot{\phi}$ and 12 *matrix conditions of connectivity* [12] and, finally, the relative velocities $\omega_{10}^A,\ v_{21}^A,\ \omega_{32}^A, \omega_{10}^B,\ \omega_{21}^B,\ v_{32}^B,\ \omega_{10}^C,\ \omega_{21}^C,\ v_{32}^C,\ \omega_{10}^D,\ \omega_{10}^D,\ v$:

$$\omega_{10}^A\vec{u}_i^T a_{10}^T\widetilde{u}_3\{\vec{r}_{21}^{\,A} + a_{21}^T\vec{r}_{32}^{\,A} + a_{21}^T a_{32}^T a_{43}^T\vec{r}_4^{\,G}\} + v_{21}^A\vec{u}_i^T a_{10}^T\vec{u}_1 + \omega_{32}^A\vec{u}_i^T a_{30}^T\widetilde{u}_3 a_{43}^T\vec{r}_4^{\,G} = \vec{u}_i^T\dot{\vec{r}}_0^{\,G}\ (i=1,2)$$

$$-\omega_{10}^A\vec{u}_j^T a_{10}^T\widetilde{u}_3 a_{21}^T a_{32}^T a_{43}^T\vec{r}_4^{\,GB_4} - \omega_{32}^A\vec{u}_j^T a_{30}^T\widetilde{u}_3 a_{43}^T\vec{r}_4^{\,GB_4} + \omega_{10}^B\,\vec{u}_j^T b_{10}^T\,\widetilde{u}_3 b_{21}^T\{\vec{r}_{32}^{\,B} + b_{32}^T\vec{r}_3^{\,B_4}\} +$$

$$+\omega_{21}^B\,\vec{u}_j^T b_{20}^T\,\widetilde{u}_3\{\vec{r}_{32}^{\,B} + b_{32}^T\vec{r}_3^{\,B_4}\} + v_{21}^B\vec{u}_j^T b_{20}^T\vec{u}_1 = \vec{u}_j^T\dot{\vec{r}}_0^{\,G} + \dot{\phi}\vec{u}_j^T a_{40}^T\widetilde{u}_3\vec{r}_4^{\,GB_4}$$

$$-\omega_{10}^A\vec{u}_j^T a_{10}^T\widetilde{u}_3 a_{21}^T a_{32}^T a_{43}^T\vec{r}_4^{\,GC_4} - \omega_{32}^A\vec{u}_j^T a_{30}^T\widetilde{u}_3 a_{43}^T\vec{r}_4^{\,GC_4} + \omega_{10}^C\,\vec{u}_j^T c_{10}^T\,\widetilde{u}_3 c_{21}^T\{\vec{r}_{32}^{\,C} + c_{32}^T\vec{r}_3^{\,C_4}\} +$$

$$+\omega_{21}^C\,\vec{u}_j^T c_{20}^T\,\widetilde{u}_3\{\vec{r}_{32}^{\,C} + c_{32}^T\vec{r}_3^{\,C_4}\} + v_{21}^C\vec{u}_j^T c_{20}^T\vec{u}_1 = \vec{u}_j^T\dot{\vec{r}}_0^{\,G} + \dot{\phi}\vec{u}_j^T a_{40}^T\widetilde{u}_3\vec{r}_4^{\,GC_4} \qquad (j=1,2,3)$$

$$\omega_{10}^A\vec{u}_i^T a_{10}^T\widetilde{u}_3 a_{21}^T a_{32}^T\vec{r}_3^{\,D_2G} + \omega_{32}^A\vec{u}_i^T a_{30}^T\widetilde{u}_3\vec{r}_3^{\,D_2G} + \omega_{10}^D\vec{u}_i^T d_{10}^T\widetilde{u}_3\vec{r}_1^{\,D_2} = \vec{u}_i^T\dot{\vec{r}}_0^{\,G} \tag{10}$$

$$\omega_{10}^A\vec{u}_i^T a_{10}^T\widetilde{u}_3 a_{21}^T a_{32}^T\vec{r}_3^{\,E_2G} + \omega_{32}^A\vec{u}_i^T a_{30}^T\widetilde{u}_3\vec{r}_3^{\,E_2G} + \omega_{10}^E\vec{u}_i^T e_{10}^T\widetilde{u}_3\vec{r}_1^{\,E_2} + v\vec{u}_i^T a_{30}^T\vec{u}_1 = \vec{u}_i^T\dot{\vec{r}}_0^{\,G} \qquad (i=1,2)\,.$$

Particularly, starting from these matrix equations we can also obtain three analytical solutions for the linear velocities of the prismatic actuators:

$$v_{21}^A = \dot{x}_0^G\cos(\varphi_{10}^A + \alpha_1) + \dot{y}_0^G\sin(\varphi_{10}^A + \alpha_1) - \omega_{30}^A h\sin(\varphi_{32}^A + \alpha_2)$$

$$v_{32}^B = [-\dot{x}_0^G\sin\varphi_{10}^B + \dot{y}_0^G\cos\varphi_{10}^B + \frac{b}{2}\omega_{30}^A\sin\phi\sin(\varphi_{10}^A - \varphi_{32}^A - \varphi_{10}^B + \alpha_1 - \alpha_2) -$$

$$-\frac{b}{2}\dot{\phi}\cos\phi\cos(\varphi_{10}^A - \varphi_{32}^A - \varphi_{10}^B + \alpha_1 - \alpha_2)]\sin(\varphi_{21}^B + \alpha_3) + \frac{b}{2}\dot{\phi}\sin\phi\cos(\varphi_{21}^B + \alpha_3)$$

$$v_{32}^C = [-\dot{x}_0^G\sin\varphi_{10}^C + \dot{y}_0^G\cos\varphi_{10}^C - \frac{b}{2}\omega_{30}^A\sin\phi\sin(\varphi_{10}^A - \varphi_{32}^A - \varphi_{10}^C + \alpha_1 - \alpha_2) +$$

$$+\frac{b}{2}\dot{\phi}\cos\phi\cos(\varphi_{10}^A - \varphi_{32}^A - \varphi_{10}^C + \alpha_1 - \alpha_2)]\sin(\varphi_{21}^C + \alpha_3) - \frac{b}{2}\dot{\phi}\sin\phi\cos(\varphi_{21}^C + \alpha_3)$$

$$\omega_{30}^A = -\frac{\dot{x}_0^G\cos(\varphi_{10}^D + \alpha_4) + \dot{y}_0^G\sin(\varphi_{10}^D + \alpha_4)}{(h - d_1)\sin(\varphi_{10}^A - \varphi_{32}^A - \varphi_{10}^D + \alpha_1 - \alpha_2 - \alpha_4)}\,. \tag{11}$$

The derivatives of theses relations lead immediately to the relative linear accelerations $\gamma_{21}^A,\ \gamma_{32}^B,\ \gamma_{32}^C$.

As an application let us consider a parallel simulator which has the following geometrical and architectural characteristics

$$x_0^{G^*} = 0.05\,m\,,\ y_0^{G^*} = 0.1m\,,\ \phi^* = \pi/12\,,\ s_A = 0.29m,\ s_B = s_C = 0.33m$$

$$A_3D_2 = d_1 = 0.4m,\ A_1E_1 = d_2 = 0.95m,\ E_1D_1 = d_3 = 0.65m$$

$$D_1F = d_4 = 0.25m, B_2F = C_2F = d_5 = 1.35m$$

$$A_2A_3 = l_1 = 0.85m,\ B_3B_4 = C_3C_4 = l_2 = 1m$$

$$D_1D_2 = l_3 = 1.3m, E_1E_2 = l_4 = 1.2m,\ B_4C_4 = b = 1.2m$$

$$A_4G = h = 1.4m,\ FG = h_G = 1.1m,\ \Delta t = 3\ s.$$

Using MATLAB software, a computer program was developed to solve the kinematics of the parallel simulator. To develop the algorithm, it is assumed that the platform starts at rest from a central configuration and moves pursuing successively some evolutions.

Three examples are solved to illustrate the algorithm.

In a first example, the platform's point G moves along the *vertical direction* y_0 with variable acceleration while all the other positional parameters are held equal to zero. The time-histories for the input displacements $\lambda_{21}^A, \lambda_{32}^B, \lambda_{32}^C$ (Fig. 3), relative velocities $v_{21}^A, v_{32}^B, v_{32}^C$ (Fig. 4) and accelerations $\gamma_{21}^A, \gamma_{32}^B, \gamma_{32}^C$ (Fig. 5) are carried out for a period of $\Delta t = 3$ seconds in terms of analytical equations (6).

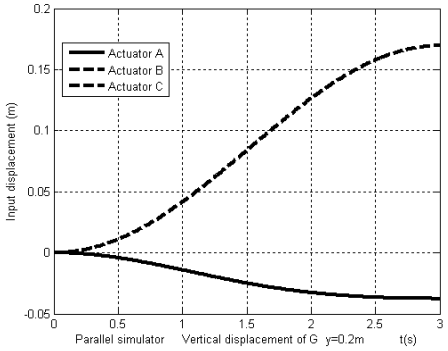

Fig. 3 Input displacements of the three sliders

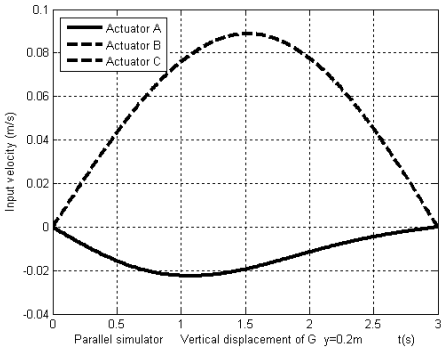

Fig. 4 Input velocities of the three sliders

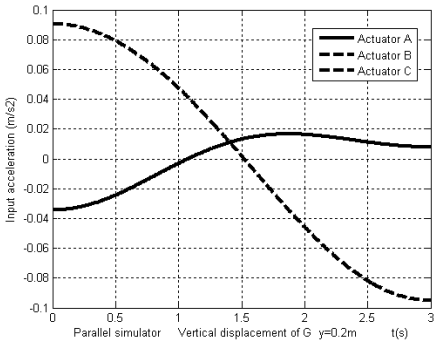

Fig. 5 Input accelerations of the three sliders

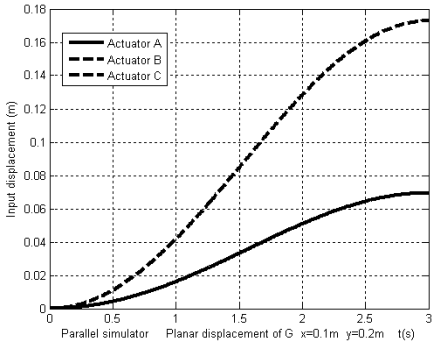

Fig. 6 Input displacements of the three sliders

For the case when the platform's point G moves along a *rectilinear trajectory* without a rotation of the platform around its median axis, the graphs are illustrated in Fig. 6, Fig. 7 and Fig. 8.

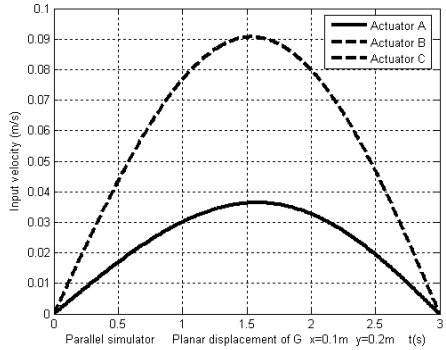

Fig. 7 Input velocities of the three sliders

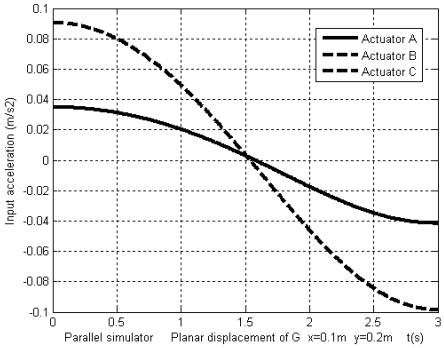

Fig. 8 Input accelerations of the three sliders

Further on, we shall consider a *general evolution* of the platform, combining a rectilinear displacement of the point G and a rotation of the platform around its median axis. Relative displacements, velocities and accelerations of three prismatic actuators are graphically sketched in Fig. 9, Fig. 10 and Fig. 11.

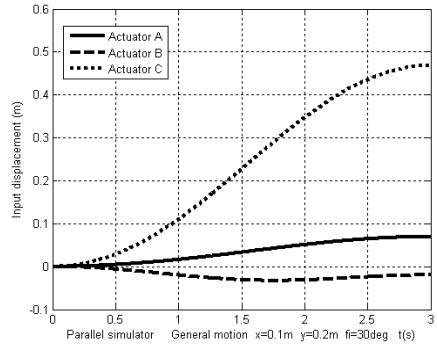

Fig. 9 Input displacements of the three sliders

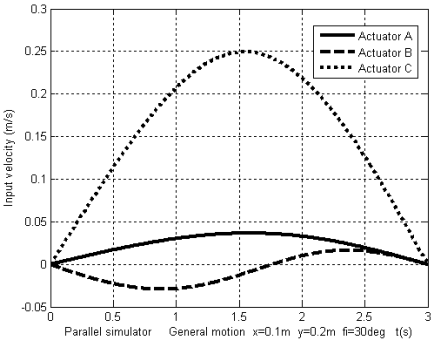

Fig. 10 Input velocities of the three sliders

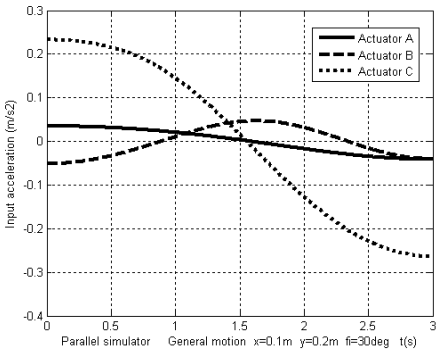

Fig. 11 Input accelerations of the three sliders

3. Conclusions

Some exact relations that give in real-time the position, velocity and acceleration of each element of a flight parallel simulator have been established in the present paper. The simulation certifies that one of the major advantages of the current matrix recursive formulation is the accuracy and a smaller processing time for the numerical computation.

Choosing the appropriate serial kinematical circuits connecting many moving platforms, the present method can be easily applied in forward and inverse mechanics of various types of parallel mechanisms, complex manipulators of higher degrees of freedom and particularly *hybrid structures*, with increased number of components of the mechanisms.

R E F E R E N C E S

[1] *Tsai, L-W.*, Robot analysis: the mechanics of serial and parallel manipulator, Wiley, 1999
[2] *Merlet, J-P.*, Parallel robots, Kluwer Academic, 2000
[3] *Stewart, D.*, A Platform with Six Degrees of Freedom, Proc. Inst. Mech. Eng., 1, 15, 180, pp. 371-378, 1965
[4] *Wang, X-C., Zhao, H., Ma, K-M., Huo, X., Yao, Y.,* Kinematics analysis of a novel all-attitude flight simulator, Science China Information Sciences, Springer, 53, 2, pp. 236-247, 2010
[5] *Karimi, D., Nategh, M.J.,* A Statistical approach to the forward kinematics nonlinearity analysis of Gough-Stewart mechanism, Journal of Applied Mathematics, Volume 2011, Article ID 393072, 17 pages, 2011
[6] *Di Gregorio, R., Parenti Castelli, V.,* Dynamics of a class of parallel wrists, ASME Journal of Mechanical Design, 126**,** 3, pp. 436-441, 2004
[7] *Pîsla, D., Itul, T., Pîsla, A., Gherman, B.,* Dynamics of a parallel platform for helicopter flight simulator considering, SYROM 2009, Visa I, Springer, pp. 365-378, 2009
[8] *Gwinnett, J.E.,* Amusement devices, US Patent No. 1789680, 1931
[9] *Ga1anov, A.S., Diaciun,V.C.,* Manipulator, URSS Patent No. 908589, 1982
[10] *Angeles, J.,* Fundamentals of Robotic Mechanical Systems: Theory, Methods and Algorithms, Springer, 2002

[11] *Staicu, S.*, Méthodes matricielles en cinématique des mécanismes, UPB Scientific Bulletin, Series D: Mechanical Engineering, 62, 1, pp. 3-10, 2000
[12] *Staicu, S.,* Dynamics of the 6-6 Stewart parallel manipulator, Robotics and Computer-Integrated Manufacturing, Elsevier, 27, 1, pp. 212-220, 2011